Dielectric Relaxations in Reduced Rutile (TiO_{2-x}) at Low Temperatures*†

L. A. K. DOMINIK‡ AND R. K. MACCRONE§
School of Metallurgical Engineering
and
Laboratory for Research on the Structure of Matter, University of Pennsylvania, Philadelphia, Pennsylvania
(Received 12 January 1967; revised manuscript received 27 July 1967)

The complex dielectric constant of reduced rutile, TiO_{2-x}, has been measured at frequencies between 10^2 and 10^5 Hz at temperatures between 1.2 and 50°K. Three distinct relaxation processes have been observed: process I at temperatures around 4.0°K with activation energy $Q=1.0\pm0.5\times10^{-3}$ eV and pre-exponential factor $\tau^*=10^{-6}$ sec, process II at temperatures around 15°K with $Q=2.0\pm0.5\times10^{-2}$ eV and $\tau^*=10^{-7}-10^{-8}$ sec, and process III at temperatures around 11°K with $Q=8.0\pm0.5\times10^{-3}$ eV and $\tau^*\approx10^{-7}$ sec. All three relaxation processes are ascribed to polaron hopping between normal cation lattice sites around complex ionic defect cores. By increasing the concentration of trivalent impurity, the most likely ionic core responsible for process I is found to be an oxygen vacancy associated with one trivalent substitutional impurity, while the core most likely responsible for process II is an interstitial Ti^{+3} ion in association with two trivalent substitutional impurity ions. An ion core consisting of a single pentavalent substitutional impurity accounts well for process III.

INTRODUCTION

CONDUCTION in *n*-type reduced rutile, TiO_{2-x}, occurs at temperatures above 30°K by the motion of electrons in a Ti^{+3} band populated by donors with energy levels $\approx10^{-2}$ eV below the bottom of the conduction band.[1–5] At lower temperatures, Hasiguti *et al.*[3,6] have observed impurity conduction similar to that observed in the elemental semiconductors.

The donors introduced by reduction, and which are responsible for the *n*-type conduction, are not well understood. The results of investigations based on the oxygen-pressure dependence of the defect state are contradictory; some results favor the oxygen vacancy as the dominant defect[7–9] while others[10,11] favor the titanium interstitial, and yet others favor a combination of the two.[12–14] Paramagnetic resonance results on reduced rutile indicate the presence of Ti^{+3} ions on normal and interstitial sites[15–17] as well as centers with unexplained spectra. Internal-friction results[18–21] cannot be explained on the basis of oxygen vacancies at all, but can be explained on the basis of associated Ti^{+3} interstitial pairs.

At temperatures below about 20°K, where the conduction band has been depopulated by the trapping of electrons in donor states in the energy gap, ac dielectric measurements yield significant information about the nature of the trapped states.

For example, an electron trapped by a positive ionic defect is most likely localized on one of a number of nearest-neighbor Ti^{+4} ion sites.[17] An electron may hop between a pair of these sites under the action of an ac field, and this hopping is equivalent to the reorientation of an electric dipole. This process would give a frequency-dependent complex dielectric constant exhibiting Debye-type behavior as has been suggested by Fröhlich, Machlup, and Mitra.[22] This is analogous to the trapping of a positive hole adjacent to a substitutional Li ion, in Li-doped nickel oxide, as proposed by Verwey.[23] ac measurements have been useful for investigating the hopping of electrons in the region of

* Supported by the Advanced Research Projects Agency of the Department of Defense.
† This work was submitted by L.A.K.D. in partial fulfillment of the requirements for the Ph.D. at the University of Pennsylvania.
‡ Present address: Providence College, Providence, Rhode Island.
§ Present address: Department of Materials Engineering, Rensselaer Polytechnic Institute, Troy, New York.
[1] R. G. Breckenridge and W. R. Hosler, Phys. Rev. **91**, 793 (1953).
[2] H. P. R. Frederikse, J. Appl. Phys. Suppl. **32**, 2211 (1961).
[3] R. R. Hasiguti, K. Minami, and H. Yonemitsu, J. Phys. Soc. Japan **16**, 2223 (1961).
[4] J. H. Becker and W. R. Hosler, J. Phys. Soc. Japan **18**, Suppl. II 152 (1963).
[5] J. H. Becker and W. R. Hosler, Phys. Rev. **137**, A1872 (1965).
[6] R. R. Hasiguti, N. Kawamiya, and E. Yagi, J. Phys. Soc. Japan **19**, 573 (1964).
[7] K. Förland, W. Buessem, T. Förland, and P. Marshall, U. S. Army Signal Corps Contract No. DA-31-039-SC, 71190 (unpublished).
[8] W. R. Buessem and S. R. Butler, *Kinetics of High Temperature Processes*, edited by W. D. Kingery (MIT Press, Cambridge, Massachusetts, 1959), pp. 13 ff.
[9] C. J. Kevane, Phys. Rev. **133**, A1431 (1964).
[10] T. Hurlen, Acta Chem. Scand. **13**, 365 (1959).
[11] D. S. Tannhauser, Solid State Commun. **1**, 223 (1963).
[12] P. Kofstad, J. Phys. Chem. Solids **23**, 1579 (1962).
[13] J. Yahia, Phys. Rev. **130**, 1711 (1963).
[14] R. D. Shannon, J. Appl. Phys. **35**, 3414 (1964).
[15] M. Date, Bussei (Tokyo) **1**, 22 (1960).
[16] P. F. Chester, J. Appl. Phys. **32**, 2233 (1961).
[17] H. J. Gerritsen, in *Proceedings of the First International Conference on Paramagnetic Resonance, Jerusalem, 1962*, edited by W. Low (Academic Press Inc., New York, 1963), p. 5.
[18] R. D. Carnahan and J. O. Brittain, J. Appl. Phys. **34**, 3095 (1963).
[19] J. B. Wachtman, Jr., and L. R. Doyle, Phys. Rev. **135**, A276 (1964).
[20] R. D. Carnahan and J. O. Brittain, J. Appl. Phys. **37**, 1808 (1966).
[21] J. B. Wachtman, Jr., S. Spinner, W. S. Brower, T. Fridinger, and R. W. Dickson, Phys. Rev. **148**, 811 (1966).
[22] H. Fröhlich, S. Machlup, and T. K. Mitra, Phys. Kondensierten Materie **1**, 359 (1963).
[23] E. J. W. Verwey, *Semiconducting Materials* (Butterworths Scientific Publications, Ltd., London, 1951), p. 151.

impurity conduction in elemental semiconductors,[24] and polaron behavior in ZnO at higher temperatures.[25]

PHENOMENOLOGICAL EQUATIONS

The complex dielectric constant $K+iK'$ of a material exhibiting a dielectric relaxation is given as a function of angular frequency ω by the well-known Debye equations[26]

$$K(\omega)-K_\infty=(K_0-K_\infty)/(1+\omega^2\tau^2),$$
$$K'(\omega)=(K_0-K_\infty)\omega\tau/(1+\omega^2\tau^2),$$

where τ is the polarization relaxation time, and K_0 and K_∞ are the dielectric constants at low and high frequencies, respectively. K_0 and K_∞ may be related by applying the Clausius-Mossotti[26] expression to a volume exhibiting several different polarization mechanisms,[27] i.e.,

$$(K_0-1)/(K_0+2)=\tfrac{4}{3}\pi(\alpha_{el}+\alpha_{ion}+\alpha_{dip})$$

at low frequencies and

$$(K_\infty-1)/(K_\infty+2)=\tfrac{4}{3}\pi(\alpha_{el}+\alpha_{ion})$$

at high frequencies, where α_{el}, α_{ion}, and α_{dip} are the electronic, ionic, and dipolar polarizability, respectively, per unit volume; α_{dip} is given by the well-known expression

$$\alpha_{dip}=n\mu^2/kT,$$

where n is the number of dipoles per unit volume of moment μ. Subtraction and rearrangement gives

$$(K_0-K_\infty)/(K_0+2)(K_\infty+2)=4\pi n\mu^2/9kT.$$

The maximum value of $\tan\delta=K'/K$, when $\omega\tau=(K_0/K_\infty)^{1/2}$, is given by

$$\begin{aligned}(\tan\delta)_{max}&=\tfrac{1}{2}(K_0-K_\infty)/(K_0K_\infty)^{1/2},\\&=(2\pi n\mu^2/9kT)(K_0K_\infty)^{1/2},\\&\approx(\pi n\mu^2/9kT)(K_0+K_\infty)\end{aligned}\qquad(1)$$

subject to the conditions K_0, $K_\infty\gg2$.

In practice a single relaxation time usually does not describe the relaxation process; rather a distribution of relaxation times is required. The theoretical description of physical models exhibiting a distribution of relaxation times is often very complex. It is sufficient for our purposes to quote the results of a simple model[26] in which the barrier heights involved for the dipolar reorientation are equally distributed between Q and $Q+v$. In this case, $\tau_0\leq\tau\leq\tau_1$, and

$$\tan\delta\approx(\tan\delta)_{max}\left\{\frac{\tan^{-1}\omega\beta/\omega_m-\tan^{-1}\omega/\beta\omega_m}{\tan^{-1}\beta-\tan^{-1}(1/\beta)}\right\},\qquad(2)$$

where ω_m is the angular frequency at which K' is a maximum and β and τ_1 are defined by

$$\beta=(\tau_1/\tau_0)^{1/2}=\exp v/2kT;\qquad(3)$$

and

$$\begin{aligned}(\tan\delta)_{max}&\approx\frac{1}{2}\frac{(K_0-K_\infty)}{(K_0K_\infty)^{1/2}}\frac{\tan^{-1}\beta-\tan^{-1}(1/\beta)}{\ln\beta}\\&=\frac{2\pi n\mu^2}{3kT}\frac{(K_0+2K_\infty)}{(K_0K_\infty)^{1/2}}\left\{\frac{\tan^{-1}\beta-\tan^{-1}(1/\beta)}{\ln\beta}\right\},\end{aligned}\qquad(4)$$

using the Clausius-Mossotti expression.

Assuming that $\tau_0=\tau^*\exp Q/kT$, the angular frequency ω_m at which K' is a maximum decreases with decreasing temperature according to the expression

$$1/\omega_m\tau^*=\exp(Q+\tfrac{1}{2}v)/kT.\qquad(5)$$

The parameter β may be determined by fitting the theoretical expression (2) to the experimentally determined $\tan\delta$-versus-ω curve in the region near the maximum, and v determined from Eq. (3). The quantity $(Q+\frac{1}{2}v)/k$ may be calculated from the shift of the dispersion maxima with temperature or frequency according to the relation

$$\ln\left[\frac{\omega_{1\,max}}{\omega_{2\,max}}\right]=\frac{(Q+\frac{1}{2}v)}{k}\left[\frac{(T_1-T_2)}{T_1T_2}\right],\qquad(6)$$

where ω_i and T_i are, respectively, the angular frequency and temperature at which a maximum in the dispersion occurs. The activation energy Q is then obtained from the known values of v and $(Q+\frac{1}{2}v)$. In practice the value of $\frac{1}{2}v$ is smaller than the experimental error in the determination of Q, and thus may be neglected. Finally, Eq. (4) may be used to determine $n\mu^2$, if the number of active dipoles is independent of temperature.

The measured values of capacity and loss are the resultants of a surface capacitance and conductance in series with the bulk capacitance and conductance[28] together with any relaxation process, as described. In the case where the bulk conductance is very small and the surface capacitance is very large, the relaxation process will dominate. The experimental results presented in this paper concern large dielectric relaxations where the above two conditions are valid. Consequently, any discussion of the dispersive behavior of an equivalent circuit, and the temperature dependence of the circuit, may be omitted entirely.

EXPERIMENTAL METHOD

Specimens in the form of disks about 1.0 cm in diam and 0.1–0.2 cm thick were cut from a Verneuil-grown boule obtained from the Linde Division of Union Carbide. The impurity content of representative material is given as follows: trivalent impurity: 0.005%

[24] M. Pollak and T. H. Geballe, Phys. Rev. **122**, 1742 (1961).
[25] D. P. Snowden and H. Saltzburg, Phys. Rev. Letters **14**, 497 (1965).
[26] H. Fröhlich, *Theory of Dielectrics* (Oxford University Press, New York, 1958), pp. 73–75, 91–98, 121–122.
[27] H. P. Layer, Ph.D. thesis, University of North Carolina, 1964, p. 34 (unpublished).
[28] R. A. Parker and J. H. Wasilik, Phys. Rev. **120**, 1631 (1960).

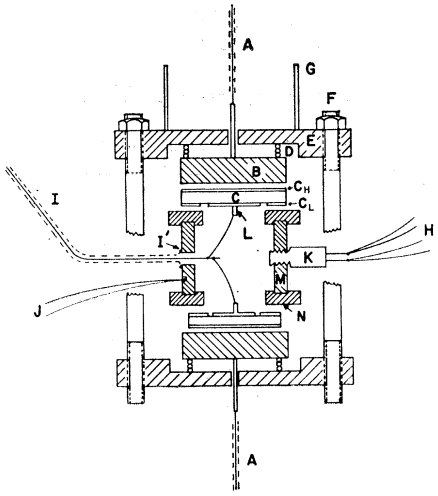

FIG. 1. Details of specimen holder. Thick-walled copper cylinder M; resistance thermometer K; see text.

Fe_2O_3, 0.005% Al_2O_3, 0.01% B_2O_3; pentavalent impurity: 0.005% V_2O_5; equi-valent impurity: 0.003% SiO_2, 0.005% SnO_2, 0.01% ZnO_2.

Specimens with three different orientations, determined by standard x-ray techniques, were prepared:

(i) plane of disk ⊥ to c axis, [001],
(ii) plane of disk ⊥ to a axis, [100],
(iii) plane of disk at 45° to both a axes, [110].

The actual orientation achieved differed by no more than 3° from the desired orientation.

The samples were reduced by heating at 900°C in a partially evacuated vycor capsule for 72 h, followed by furnace cooling at a rate of 200°C/h. It has been found, however, that the relative degree of reduction obtained by this method cannot be reliably deduced from the oxygen partial pressure: Even specimens reduced in the same capsule differ among themselves. A more reliable measure of the degree of reduction is based on the assumption that the electronic conduction at room temperature is proportional to the number of ionic defects introduced during reduction. Thus four-terminal dc resistivity measurements, using the van der Pauw[29] method, were made at room temperature. This quantity, together with the literature value for mobility, namely, 1.0 cm^2/V sec,[5,6] enables the carrier density, or degree of reduction, to be determined. The details of the specimens, their reduction pressure and carrier concentration as determined from the electrical resistivity by this method are given in Table I. In addition, to validate the above method, the Hall coefficient was measured by a standard potentiometric technique on two specimens at 77°K, and the resulting carrier concentrations obtained are also given in Table I. (The Hall coefficient at room temperature was too small to measure with the available equipment.) The agreement between the carrier concentrations obtained directly from Hall measurements and those obtained indirectly using the literature value for the mobility is most satisfactory, as shown in Table I.

TABLE I. Details of specimens, reduction pressures and resulting carrier densities.

Specimen	Reduction pressure, μ Hg (300°K)	$n_{300°K}$ (10^{18} cm^{-3})	$n_{78°K}$ (cm^{-3}) (i)[a]	$n_{78°K}$ (cm^{-3}) (ii)[b]
A	25	1.86		
B	50	1.42		
C-Fe-1	50	···		
D	90–100	1.03		
E	90–100	0.59		
G	0.045	1.74	$1.27-5.07\times10^{17}$	3.29×10^{17}
H	430	1.42	$1.26-5.03\times10^{17}$	3.01×10^{17}
I	$4-5\times10^3$	$<10^{-8}$		
K	0.17	···		
L[110]	90	2.63		
M[100]	90	1.57		
N[001]	90	1.29		
P	As cut, stoichiometric	$<10^{-8}$		
α	25	2.08		
γ	75	1.48		
δ	125	0.86		

[a] Calculated from experimentally measured resistivity and extrema in literature values for the Hall mobility at 78°K.
[b] Obtained directly from Hall-coefficient measurements at 78°K.

Most of the measurements reported here were made with gold electrodes, prepared by painting Du Pont gold paste No. 5780 onto the specimen surface. After curing at 200°C, these electrodes survived repeated thermal cycling between 2 and 300°K. To specifically test for surface effects, silver and nickel electrodes were also used.

The dielectric measurements were made using three terminals with a General Radio 1615-A transformer ratio arm bridge, operating at frequencies between 0.2 and 100 kHz. This bridge has the advantage that stray capacitance and loss between ground and the leads to the active plates do not significantly affect the absolute values measured. Relative changes in capacitance of 0.01 pF and changes of 0.001 in tanδ could easily be measured.

For the capacitance measurements, two samples at a time were placed in a specially constructed specimen holder, shown in Fig. 1. The central portion of the device consisted of a thick-walled copper cylinder about 5 cm long, the inside diameter being larger than the guarded center electrode of each specimen. The specimens, one at each end, were spring loaded against the cylinder so that the very wide guard ring of the specimen made good electrical and thermal contact with the copper cylinder. The lead from the guarded center electrode was brought out through suitable small holes in the wall of the copper cylinder. The sequence [spring (D)—electrode (B,C_H)—specimen (C)—guarded electrode + guard ring (C_L)—copper cylinder (M)—mirror image] was sandwiched together between Teflon disks, 0.5 cm thick, and supported vertically in a cryostat vacuum chamber in a helium atmosphere. Dielectric

[29] L. J. van der Pauw, Philips Res. Rept. 13, 1 (1958).

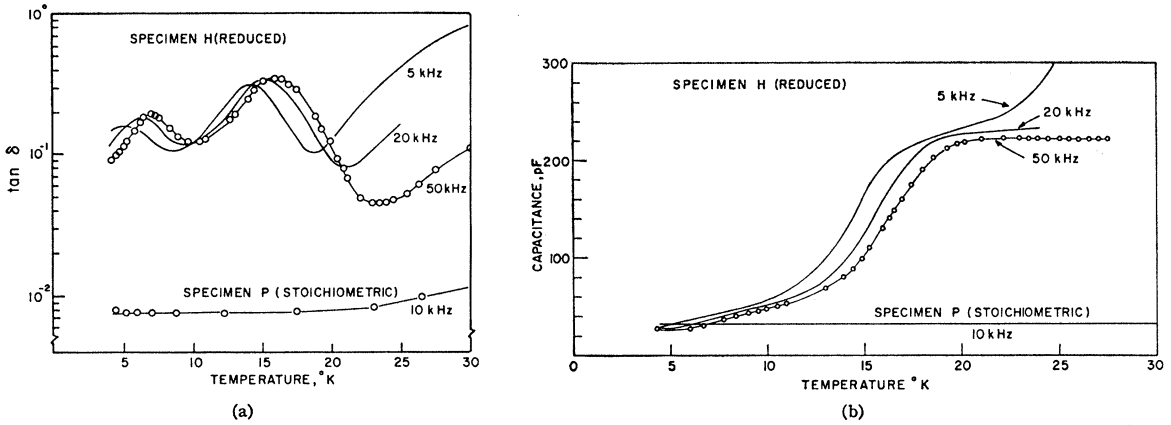

FIG. 2. Typical dielectric loss and capacitance behavior as a function of temperature, showing two relaxation processes.

measurements as a function of temperature were made by allowing the cryostat to warm up slowly from 4.2°K. A suitable warming rate, 0.2°K/min, was obtained by surrounding the vacuum chamber with charcoal.

During the electrical measurements, the guard ring and associated copper cylinder remain at earth potential. The copper cylinder provided a convenient site for the Germanium resistance thermometer (4.2–30°K) and copper-constantin thermocouple (30–300°K) used in the temperature measurement. The vapor pressure of He^4 was used to determine temperatures below 4.2°K. Since continuous heat flow to the specimens is involved, the maximum temperature difference between the thermometers and specimens was estimated. The heat flow to the specimens through the copper cylinder was overestimated by setting it equal to the observed liquid-helium boil-off rate. Assuming that a thin layer, 0.01 cm thick, of small thermal conductivity, $\frac{1}{10}$ that of copper, at the specimen-cylinder interface dominates the heat flow, the temperature difference between the copper cylinder and the specimen was found to be less than 10^{-2}°K, which is less than the accuracy to which the temperature of the maxima in the dielectric loss could be determined.

RESULTS

Figure 2 shows the typical dielectric behavior of reduced TiO_{2-x} specimens in the temperature range 4.2–

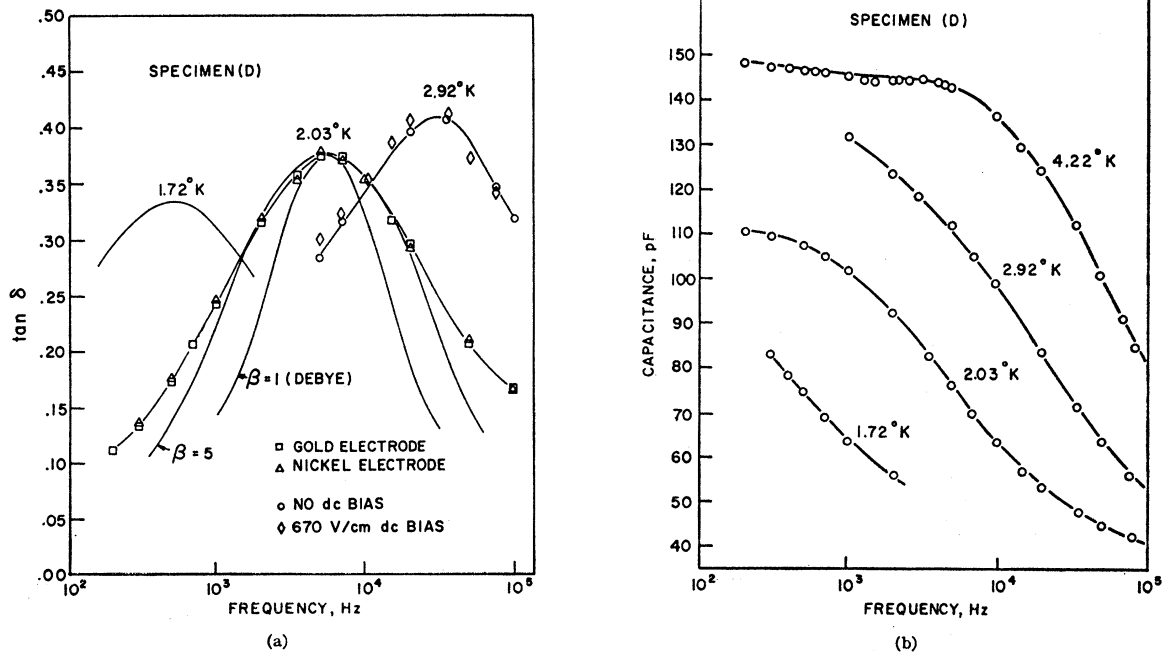

FIG. 3. Typical dielectric loss and capacitance behavior of process I as a function of frequency.

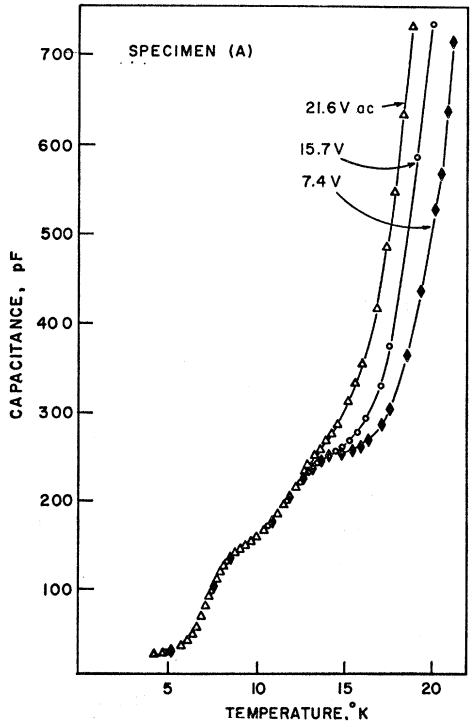

FIG. 4. The surface capacitance increase as a function of temperature and measuring voltage.

30°K. Two distinct peaks are seen. These are relaxation processes since the relation between $(\tan\delta)_{\max}$ and the associated change in dielectric constant, given by Eq. (1) for an undistributed relaxation, is found to be reasonably obeyed. The low-temperature peak, process I, exhibits a maximum in $\tan\delta$ at 20 kHz at 6.5°K, while a second process, process II, exhibits its maximum at the same frequency at 15°K. These relaxations may also be followed with frequency as the variable and temperature as the parameter. Figure 3 shows the behavior of process I as a function of frequency at various temperatures. The dispersion curves, see Fig. 3, have been analyzed for the distribution of relaxation times involved. For process I, a good fit with Eq. (2) is obtained with $\beta \approx 5$, while for process II the dispersion is broader, the best fit being obtained with $8 \leq \beta \leq 12$.

Previous measurements of the dielectric constant of reduced rutile at low frequencies by Parker and Wasilik[28] have indicated that at temperatures above 77°K, the dielectric behavior of the bulk material is obscured by the Schottky[30] exhaustion layer at the electrodes. Thus, to determine to what extent the low-temperature dielectric behavior shown in Figs. 2 and 3 depends on "surface effects," various tests for surface origin were performed. The tests were:

(i) application of a dc bias to the specimen,
(ii) use of different electrode materials,
(iii) variation in the ratio of surface area to thickness.

[30] W. Schottky, Z. Physik **118**, 539 (1942).

All of these tests indicated that the processes responsible for the two peaks are of bulk origin.

In Fig. 3, for example, the negligible effect of a dc field of 670 V/cm on process I is shown. This is very strong evidence that a Schottky barrier is not involved. Also shown in Fig. 3 is the negligible effect of different electrode materials on the relaxation. The similarity between the results obtained with gold and silver is not very conclusive, since these metals have similar work functions, and, moreover, the surface states of the TiO_2 may be the determining factor. However, Breckenridge and Hosler[31] have shown that the rectifying barrier under a nickel electrode is very different to that under a gold electrode. Therefore, the similarity between the dielectric behavior with gold and nickel electrodes strongly suggests that surface effects are not involved. Finally, anticipating the experimental result in Fig. 6, the bulk or surface origin of process I may be found by determining whether the change in capacitance of the relaxation follows the bulk expression $\Delta C = KA/d$ or the surface expression, $\Delta C = K_S A$, where K_S is a fictitious "surface dielectric constant." A least-squares analysis of the ΔC's obtained from various specimens gave a bulk dielectric constant $K = 85.9$ with abscissa intercept 22.3 with a standard deviation of 30.3. A similar analysis for the surface dielectric constant gave $K_S = 1015.6$ with abscissa intercept $+40.8$ with a standard deviation of 76.7. The mean-square analysis of the results clearly indicates the bulk origin of process I. Process II is also inferred to be of bulk origin.

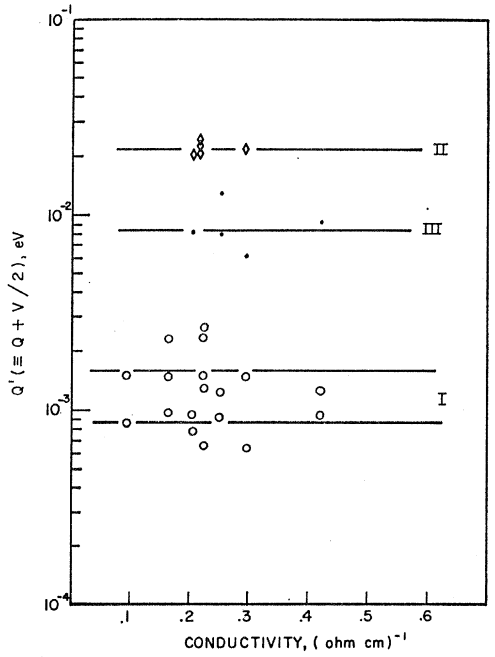

FIG. 5. The activation energies of processes I, II, and III as a function of room-temperature conductivity.

[31] R. G. Breckenridge and W. R. Hosler, J. Res. Natl. Bur. Stds. (U. S.) **49**, 65 (1952).

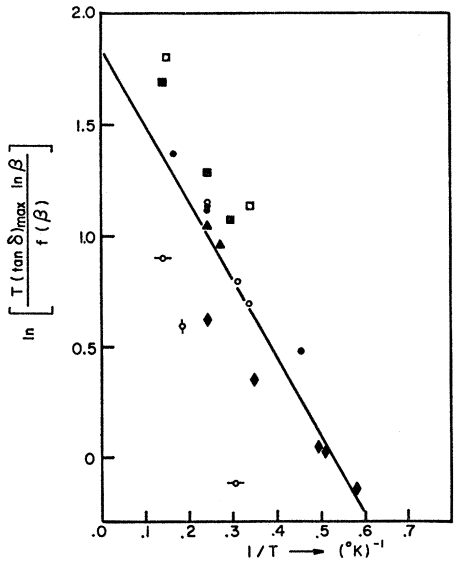

FIG. 6. $\ln[T(\tan\delta)_{\max}(\ln\beta)/f(\beta)]$ versus $1/T$ of process I for all specimens from one boule. See text.

In contrast to the relaxation processes shown in Fig. 2, and which are of bulk origin, a presumed surface capacitance effect which increases rapidly with temperature, and whose value depends on the measuring voltage and bias voltage, was also observed; this is shown in Fig. 4. Above about 20°K for fields parallel to the c axis, the surface-capacitance effect completely dominates the dielectric behavior. Apart from limiting the maximum temperature at which relaxations may be observed, the surface capacitance is of no immediate consequence to the subject of this paper and will be discussed elsewhere.

The activation energy for the dispersions may be calculated from curve fitting and Eq. (6). Figure 5 shows the values of Q for all specimens plotted as a function of the room-temperature conductivity σ. Within experimental error, the activation energy is independent of the reduction state of the specimens.

For process I, τ^* is found to be $1-2\times10^{-6}$ sec, while for process II, $\tau^*\approx10^{-7}-10^{-8}$ sec.

The value of $(\tan\delta)_{\max}$ increases without exception with increasing temperature, see Fig. 3. Equation (4), applicable to a fixed number of dipoles, predicts that $(\tan\delta)_{\max}$ will decrease slowly with increasing temperature. The experimental behavior, however, can be empirically described by the *ad hoc* assumption that K_0-K_∞ is thermally activated in some way, so that in Eq. (4) n is effectively replaced by $n_0\exp(-\Delta E'/kT)$; K_∞ is essentially independent of temperature, see Fig. 2. The modified equation becomes

$$(\tan\delta)_{\max}=\frac{\pi n_0\mu^2}{9kT}(K_0+K_\infty)e^{-\Delta E'/kT}\frac{\tan^{-1}\beta-\tan^{-1}(1/\beta)}{\ln\beta}.$$

The physical basis for this modification, and meaning of "thermal activation" in this case, is taken up in detail in the discussion.

With the notation $f(\beta)=[\tan^{-1}\beta-\tan^{-1}(1/\beta)]$ and neglecting the relatively slow temperature variation of K_0+K_∞, the above equation may be written

$$\ln\left[\frac{T(\tan\delta)_{\max}\ln\beta}{f(\beta)}\right]=\ln\left[\frac{\pi n_0\mu^2(K_0+K_\infty)}{9}\right]-\frac{\Delta E'}{kT}. \quad (7)$$

For process I, the experimentally determined values of $\ln[T(\tan\delta)_{\max}(\ln\beta)/f(\beta)]$ versus $1/T$ are shown for all specimens in Fig. 6; a good straight line is obtained. The activation energy $\Delta E'$ in Eq. (7) obtained from the slope was found to be $3.0\pm0.5\times10^{-4}$ eV. The intercept yielded a value from which, using a dipole moment appropriate to the oxygen vacancy (Fig. 12), the value of n_0 was found to be $5\times10^{16}<n_0<5\times10^{17}$, the uncertainty being introduced mainly by the difficulty involved in extracting values for K_0 and K_∞ within the limited frequency range available. The peak height for process II also increases with increasing temperature. However, the limited temperature range within which process II was observed precludes the possibility of a similar analysis. The similarity between processes I and II implies that an equation of the form (7) also describes

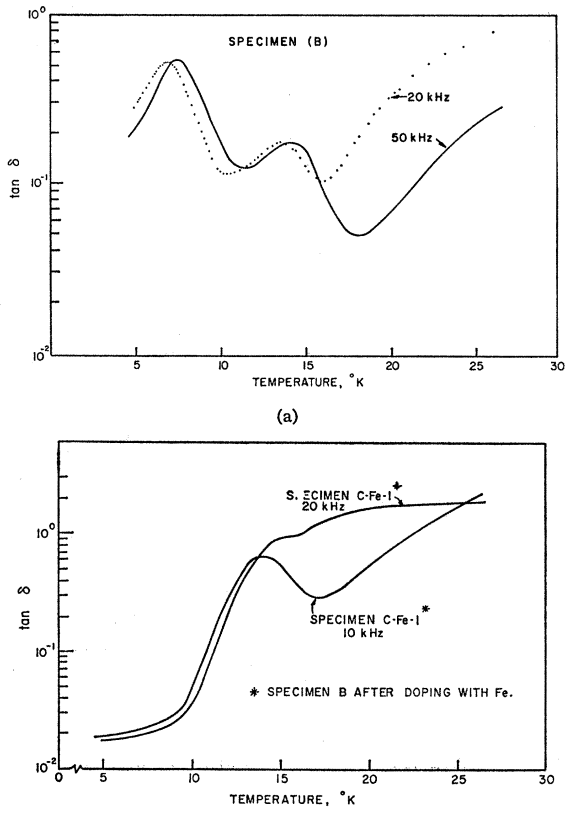

FIG. 7. Dielectric behavior of specimen B before (a) and after (b) doping with Fe.

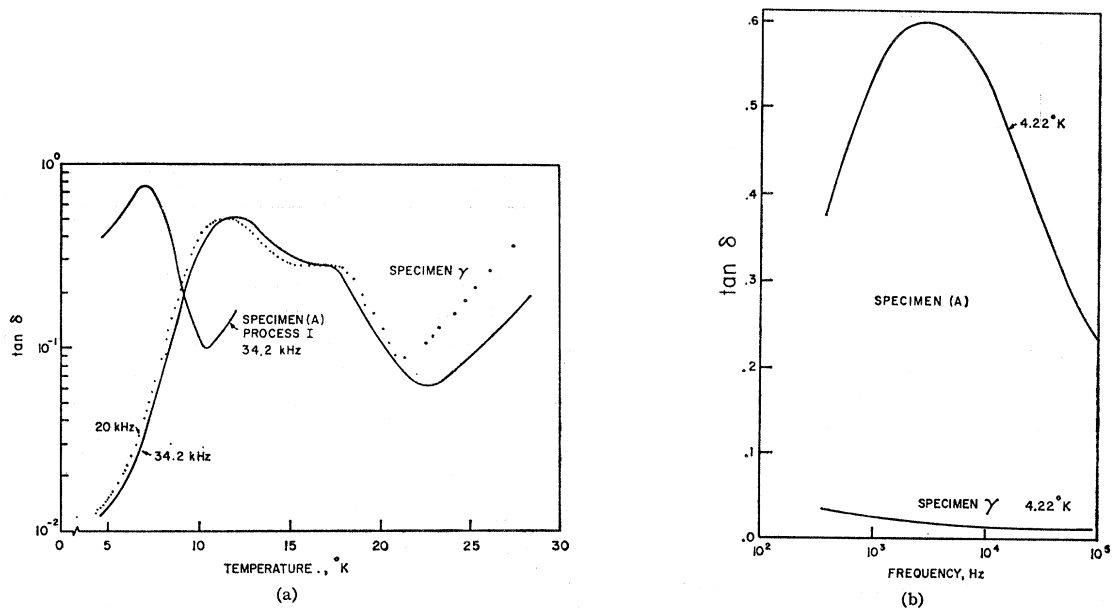

FIG. 8. Dielectric behavior of specimen γ from second boule as a function of temperature (a) and frequency (b). Typical behavior of previous boule shown for comparison.

process II; the number of active dipoles involved is certainly comparable with process I.

[It is interesting to consider how closely the Clausius-Mossotti catastrophe is approached; it occurs when $\frac{4}{3}\pi\alpha_{\text{dip}}=4\pi n\mu^2/3kT=1$. The greatest value of $\frac{4}{3}\pi\alpha_d$ calculated for the experimental conditions in this work was 10^{-1}, generally values $\approx 10^{-2}$ obtain. The use of the Clausius-Mossotti expression is thus a reasonable approximation.]

Since the experimental data for specimens of different reduction states are all fitted by a single line (Fig. 6) the value of n_0 obtained from Eq. (7) must be related to the extrinsic impurity concentration N_a rather than to the intrinsic and variable donor concentration N_d, the number of defects introduced by reduction. This conclusion can also be drawn from the extraction of a bulk dielectric constant for process I from specimens of different reduction states, as previously discussed.

To test this hypothesis, a trace of high-purity iron powder was dusted onto the surface of a previously measured specimen which was then reduced in the usual way. The dielectric behavior of the specimen before and after the doping treatment is shown in Fig. 7. [It has been established that successive reduction does not affect the behavior: the difference between Eqs. 7(a) and 7(b) is solely due to the higher impurity content.]

The magnitude of process I was vastly decreased by this treatment, while the magnitude of process II was considerably increased. This behavior indicates that the defects responsible for the relaxations are compound defects formed probably from the association of substitutional impurities with reduction defects. The increase of the magnitude of process II at the expense of process I has two alternative explanations, namely,

(i) that the impurity combines with the defect responsible for process I to form a new defect responsible for process II, or

(ii) that the impurity renders the defects responsible for process I inoperative by combination or by clustering in some way, and the impurities also increase the number of defects responsible for process II independently.

The dependence of processes I and II on extrinsic impurity content was further investigated by using specimens from a different boule. The typical behavior of a reduced specimen from this new boule is shown in Fig. 8. Process II is about the same magnitude as before while process I is absent. This difference in behavior indicates that the second boule contains more trivalent impurity (see Fig. 7).

The dielectric behavior of the second boule (Fig. 8) clearly shows, in addition, the existence of another process, process III at 11°K at 20 kHz. This peak is also exhibited by specimens from the first boule, but is very much smaller, and is often obscured by the larger peaks I and II previously described.

The orientation dependence of the three processes was investigated by using specimens whose disk planes were either (100) or (110). [All previous measurements were carried out on disks whose plane was (001)]. The results for the (110) specimen are shown in Fig. 9 together with the typical (001) behavior for easy comparison. The results for the (100) specimen are shown in Fig. 10. The significant features are:

(i) Peak I (5°K) is larger and narrower for fields along the [100] and [110] directions than along the [001] direction.

(ii) Peak II ($\approx 16°K$) does not appear for fields along [100] and [110].

(iii) Peak III ($\approx 11°K$) does not depend strongly on field direction. (Notice how in Fig. 9. Peak III on the [001] crystal appears only as a knee in the loss curve.)

(iv) The surface capacitance for fields parallel to [100] and [110] is absent.

The activation energy obtained for processes I and III with fields parallel to [100] and [110] are the same, within experimental error, as the values obtained when the electric field is parallel to [001].

DISCUSSION

The possibility that the dielectric relaxations described here are due to ion jumping is immediately ruled out by comparing the activation energies involved. The dielectric relaxations have activation energies $\approx 10^{-3}$ eV (process I) and $\approx 10^{-2}$ eV (process II), compared to ≈ 0.3–1.0 eV for ion jumping deduced from mechanical relaxation obtained by Carnahan and Brittain[18,20] and Wachtman *et al.*,[19,21] who describe their results in terms of Ti^{+3} interstitial ions hopping in complex centers. The activation energies involved here are comparable to the dc impurity conduction activation energies of Hasiguti *et al.*[6] ($\approx 10^{-3}$ eV) and are smaller than the conventional activation energy for conduction[1–5] by a reasonable factor. The relaxations are therefore ascribed to electronic motion.

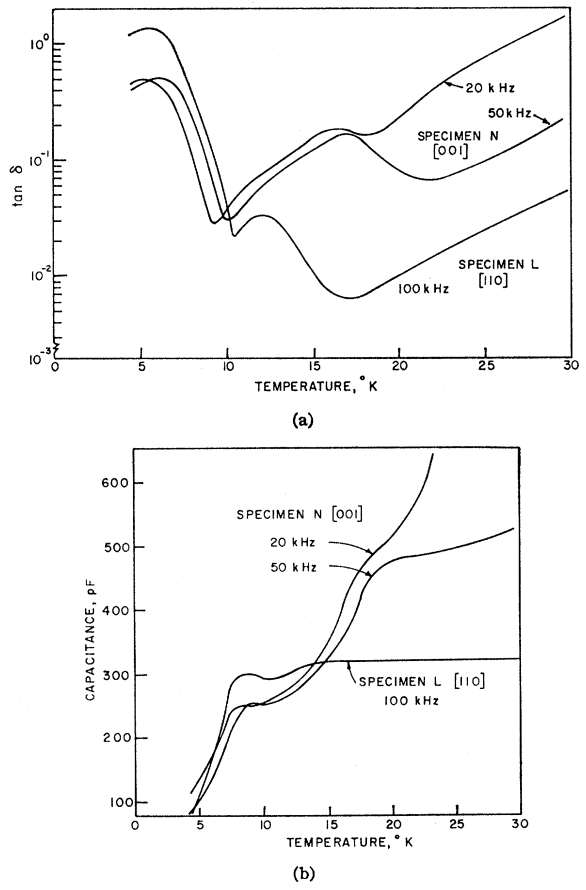

FIG. 9. Dielectric behavior of [110] specimen. The typical behavior of a [001] specimen is included for comparison.

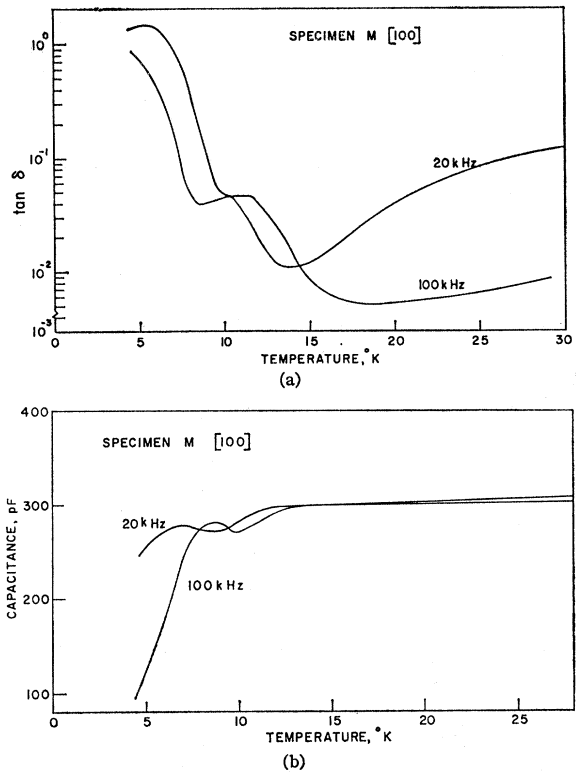

FIG. 10. Dielectric behavior of [100] specimen.

At low temperatures the positively charged ionic defects introduced by reduction trap electrons. The model proposed to explain the dielectric behavior assumes that the electron(s) of the neutral defect are localized on normal Ti sites of the lattice adjacent to the positive ionic defects and are not in conventional hydrogenic states with an effective mass. There will be several equivalent lattice sites available, related to the crystal symmetry, and between which the electron may hop. These electron hops are equivalent to the reorientation of electric dipoles, and if the rate at which an ensemble of these centers approaches the equilibrium nonpolar configuration after a disturbance is characterized by an exponential relaxation time τ, a Debye dispersion behavior is to be expected. The actual lattice sites involved between which electron hopping occurs will depend upon the ionic defect center itself, i.e., whether electron hopping occurs across an oxygen vacancy or titanium interstitial, or an associated defect complex.

The Localized Electron States

The critical assumption on which the proposed model is based is that, at low temperatures, an electron be-

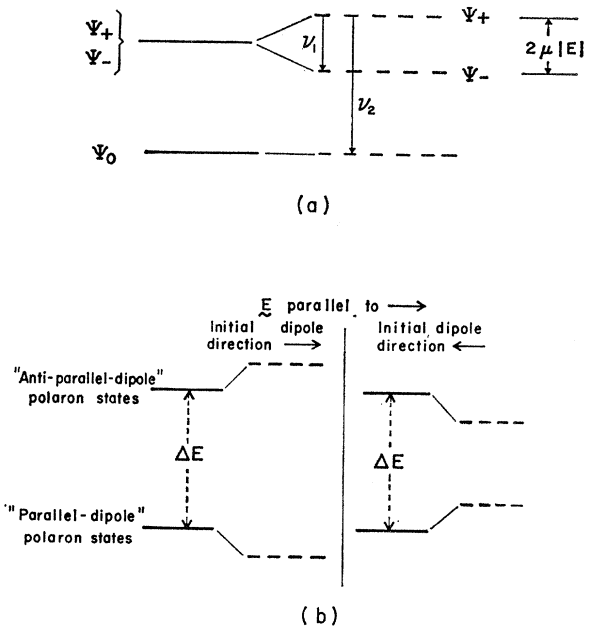

FIG. 11. Schematic energy levels, see text. (a) Electron energy levels. (b) Polaron energy levels. $E=0$ solid lines, $E=E$ dotted lines.

comes localized in some state on normal Ti^{+4} sites to form Ti^{+3} ions. The Ti^{+3} ion then acts as the effective negative charge of the electric dipole of the defect center.

The most direct evidence for electrons localized on normal lattice sites is obtained from the symmetry of the paramagnetic resonance spectra of Date[15] and of Gerritsen.[17] The spectra obtained indicate that in addition to interstitial Ti^{+3} ions, also observed by Chester,[16] there are indeed Ti^{+3} ions on normal crystallographic sites.

On general grounds, the Bohr radius of the ground state is expected to be of the order of the lattice spacing, and not of large radial extent as encountered in the elemental semiconductors, the small radius being due to the large effective mass encountered in oxides and the small dielectric constant expected at frequencies sufficiently high that no lattice polarization occurs. In addition, if hydrogenlike states of large radial extent were present in reduced rutile, there would be, by comparison with elemental semiconductors of comparable impurity concentration, more than sufficient overlap of the wave functions to produce temperature-independent metallic-impurity conduction. This mode of conduction has not been observed in rutile,[6] and is taken to be indirect experimental evidence that hydrogenic donor states of large radial extent are not present at low temperatures. The low value of the Hall mobility is also consistent with this view.

The simplest model to consider is that of an electron moving in the potential of two *equivalent* positive ions, namely the cations between which electron hopping gives rise to the dielectric relaxations. An order of magnitude estimate of the jump frequency based on this "equivalent-cation" model is, as shown below, several orders of magnitude greater than that experimentally observed, and would not give rise to the Debye dispersions observed here at kHz frequencies. For this reason a polaron model is proposed. In this model the positive ions are *inequivalent* because of the ionic displacements accompanying lattice polarization. The polaron model, as shown below, leads to a satisfactory explanation of the experimental results.

Consider first the model based on two equivalent cation sites, in particular the equivalent cation sites (i) and (ii) associated with the oxygen vacancy shown in Fig. 12(b). (This defect is later shown to be involved with peak I). The ground-state electron wave function is either symmetric or antisymmetric, and both these wave functions have a charge density equally distributed between the two cation sites. Dipole reorientation does not occur for transitions between such states. However, dipolar reorientation will be involved for transitions between ground states of the above type, whatever their form, and excited molecular orbital states, say, of the type

$$\psi_+=\psi_1(r-a)+\psi_2(r-b),$$

where the first term on the right-hand side is a ground-state wave function centered on the cation site (i), while the second an excited-state wave function centerd on the cation site (ii), Fig. 12(b). This type of dipole reorientation is schematically represented by the equation $\psi_0 \rightarrow \psi_+$. Dipolar reorientation will also be involved for direct transitions between the excited states ψ_+ and ψ_-, where ψ_- is defined as

$$\psi_-=\psi_2(r-a)+\psi_1(r-b).$$

The energy-level scheme in the absence (solid lines) and presence (dotted lines) of an electric field E parallel to the direction of dipolar reorientation is schematically indicated in Fig. 11(a). A net polarization in the presence of an electric field results from the greater population of state ψ_- compared to ψ_+ for the given field direction.

Of paramount importance in determining the applicability of the above equivalent cation model, which neglects the effects of lattice polarization, is the relaxation time τ with which equilibrium is approached after the sudden application (or removal) of a steady electric field. Let the direct transition rate ψ_+ and ψ_- be $\nu_1=1/\tau_1$ sec^{-1}, and the indirect transition rate $\psi_+ \rightarrow \psi_0 \rightarrow \psi_-$ be $\nu_2=1/\tau_2$ sec^{-1}. We estimate ν_2, the transition probability from the excited state to the ground state crudely using the expression $\nu_2=\nu_0 \exp(-E/kT)$ with $\nu_0 \approx 10^{13}$ sec^{-1}. This gives $\nu_2 \approx 10^{12}$ sec^{-1} at $T=2$°K for $E \approx 10^{-4}$ eV. [The expression $\nu_2=(2\pi/\hbar)|H_{ij}|^2$ would only be realistic if the wave functions ψ_i and ψ_j were accurately known.] The value estimated above is probably within a few orders of magnitude and repre-

sents the lower limit of the transition rate, i.e., the case where $\nu_1=0$. Equilibrium will be achieved at a more rapid rate whenever $\nu_1>0$. In any event, the lower limit ν_2 as estimated above is orders of magnitude larger than the experimentally observed transition rates, 10^6 to 10^8 sec^{-1}. The estimated value of ν_2 indicates that the above model, which does not take the lattice polarization into account, is untenable.

Consider next the case where the lattice polarization removes the equivalence of sites (i) and (ii), Fig. 12(b). Suppose the electron is localized on site (i) in a polaron state. If the electron should hop to site (ii), which is equivalent to a dipole reversal together with a small translation, it will find itself in a state of higher energy. This is so because the second electrostatic configuration involves a now antiparallel dipole in the lattice polarization field induced by the then parallel dipole. Of course, this lattice polarization will decay and reverse direction with a characteristic relaxation time, so that ultimately the electron on site (ii) will have the same energy as it had originally when on site (i). We shall call the original electron state on site (i) (or on site (ii) after a time long compared to the lattice relaxation time) the "parallel-dipole" polaron state, and the electron state immediately after the hop, before any lattice relaxation, the "antiparallel-dipole" polaron state. Let the energy difference between these two polaron states be ΔE. The energy-level scheme for the two different dipole directions is shown in Fig. 11(b) in the absence of a static electric field (solid lines) and in the presence of a static electric field (dotted lines).

A straightforward statistical analysis of the above energy scheme leads to the expression

$$(K_0-K_\infty)/(K_0+2)(K_\infty+2)=(4\pi n_0\mu^2/kT)e^{-\Delta E/2kT}.$$

If in the attainment of equilibrium the polarons hop over a distribution of barrier heights into the levels of higher energy (the antiparallel-dipole polaron states), Eq. (7) is obtained with $\Delta E=2\Delta E'$, provided the distribution of relaxation times is described by Eq. (2). The agreement between the experimental behavior and Eq. (7), as shown in Fig. 6, is thus strong evidence for the hopping of polarons at low temperatures. Polaron formation in rutile at low temperatures has been suggested by Frederikse *et al.*[32]

Structure of Ionic Defects

The values of $(\tan\delta)_{max}$ for all three dielectric relaxation processes do not depend simply on the state of reduction of the specimen, i.e., on the intrinsic donor concentration. This indicates that extrinsic impurities are involved in some way. Indeed, using specimens of different size and with differing degrees of reduction but from the same boule, it was possible, as has been mentioned, not only to verify that peak I was of bulk origin but also to show that the magnitude of the process was due to a fixed impurity concentration, Fig. 6. The direct experimental evidence for the dependence of peak height on impurity concentration is shown in Fig. 7. The decrease of peak I with increasing impurity concentration strongly suggests that a new complex defect is being formed from that responsible for peak I, which may itself be an associated complex. The complex defect centers involved are likely to be formed from the association of the intrinsic donor defects (O_v^{-2} or Ti_{int}^{+3}) with trivalent extrinsic impurities, (Al^{+3}, Fe^{+3}, B^{+3}) the major substitutional impurity types present in commercial boules. This association between intrinsic and extrinsic impurities must be assumed since the increase of one peak at the expense of another cannot be explained in terms of isolated defects alone. For example, suppose a particular relaxation process be due to the compensation of the majority donors. In this case the relaxations due to donors missing one (or more) electron or acceptors with one (or more) electron would be expected to increase monotonically with increasing acceptor concentration for the case $N_d \gg N_a$, appropriate to the n-type specimens here. That this behavior is not observed renders the above assumption untenable.

The dielectric relaxations only appear on reduction. Their absence in the "stoichiometric" material[33] of very

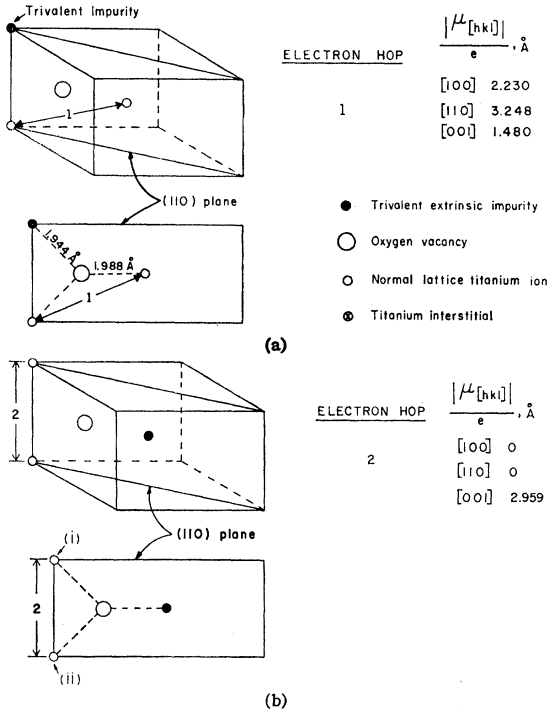

FIG. 12. Oxygen vacancy with one associated trivalent impurity in two configurations: (a) Both **a** and **c** components of μ. (b) Only **c** component of μ.

[32] H. P. R. Frederikse, W. R. Hosler, and J. H. Becker, in *Proceedings of the International Conference on Semiconductor Physics, Prague 1960* (Academic Press Inc., New York, 1961), p. 868.

[33] Here "stoichiometric" rutile is taken to refer to material with a room-temperature conductivity of less than about 10^{-10} $(\Omega\,\text{cm})^{-1}$, say.

high resistivity at room temperature indicates that the complex defects, provided they already exist, are empty acceptors with electron states lying well above the valence band or donors partly ionized by "freeze out" at low temperatures. The experimental evidence indicates that stoichiometric impure rutile is compensated during growth, and that, in consequence, association between impurities and intrinsic donor defects has probably occurred in stoichiometric, nonconducting rutile. Haul and Dümbgen[34] have found that the oxygen self-diffusion coefficient is independent of the ambient oxygen pressure, indicative that the oxygen-vacancy concentration depends rather on the extrinsic impurity concentration. Kofstad's[12] results similarly show that impurities dominate the intrinsic defects (oxygen vacancies in this case) at low concentrations, while Wachtman *et al.*[21] find intrinsic defects (titanium interstitials in this case) in nonconducting (at room temperature) Cr^{+3} doped stoichiometric rutile. Van Keymeulen[35] showed that an ionic dielectric relaxation at $\approx 400°K$, ascribed to a Fe^{+3}-oxygen vacancy complex did not occur when the specimen was quenched from 900°C, at which temperature the complex was presumably unassociated. This indicates that cooling rate is an important parameter in determining the ionic-defect state in rutile.

The internal friction results of reduced rutile are explained in terms of even more complex associated defects, namely an associated pair of cation interstitials, possibly associated in addition with a pair of trivalent ions on substitutional sites. The possibility therefore exists that the low temperature 2–30°K dielectric relaxations and the high temperature 300–700°K mechanical (and dielectric) relaxations are complimentary in a novel way. An ionic anelastic reorientation often involves dipolar reorientation and the correlation of the ionic terms is usually considered. The low temperature dielectric relaxations here are due to trapped electrons hopping around the stationary ionic center, which at the higher temperatures may give rise to a mechanical relaxation due to the reorientation of the ionic core itself. In both cases the ionic core may be the same. The possible correlation here must not be confused with the ionic rearrangements usually considered. The greater sensitivity of dielectric measurements, made in addition at low temperatures, might detect defects at concentrations too small to be detected by mechanical loss measurements, indicating that any correlations should be drawn with caution.

The qualitative dielectric behavior expected of an electron hopping between Ti^{+4} normal sites around a complex center is based on the following general considerations. Firstly, there exist groups of possible lattice sites, each member of a group having the same electrostatic energy ϵ_i (on distance considerations only), the energy of each group, however, differing from the next. The occupancy of electrons in each group is proportional to the Boltzmann factor $\exp(\epsilon_i/kT)$. It is assumed that $\epsilon_0/kT \ll \epsilon_1/kT \cdots$ etc., so that at low temperatures only occupancy of the group of lowest electrostatic energy, i.e., nearest-neighbor sites, is significant. Secondly, the transition probability for an electron hop from occupied cation to unoccupied cation site depends upon the overlap of the wave functions centered on the respective sites.[22,36] Hops over large distances are thus not favored.

The ion cores of the complex defects responsible for the dielectric relaxations which are reasonable to consider are:

(i) oxygen vacancy in association with one or more trivalent impurities,

(ii) titanium interstitial in association with one or more trivalent impurities, and

(iii) two associated titanium interstitials in association with two trivalent impurities. This defect has been proposed by Wachtman *et al.*[21] to explain internal friction behavior.

Oxygen Vacancy with One Impurity

The trivalent impurity may occupy two unequivalent lattice positions as shown in Fig. 12(a) and (b). Each of these ion configurations has a net positive charge and may in consequence trap one electron. For the ion core configuration shown in Fig. 12(a) the possible electron hop is indicated. This hop has associated a dipole-moment component in both the **a** and **c** directions, with $|\mu_a|/|\mu_c| = 2.273$. For the ion configuration shown in Fig. 12(b) the possible electron hop indicated has a component in the **c** direction only of magnitude $|\mu_c|/e = 2.959$ Å.

Oxygen Vacancy with Two Impurities

The two trivalent impurities occupy sites on either side of the oxygen vacancy, the sites of the type shown in Fig. 12(a) having lower electrostatic energy than those in Fig. 12(b). The net charge of both ionic configurations is zero; the center cannot trap an electron and will not be electronically active as a dipole.

The Titanium Interstitial Ti^{+3} Associated with Two Impurities

The nearest-neighbor positions for the trivalent impurities are shown in Fig. 13(a). This ion core has a net positive charge of one and may trap one electron. There are two possible electron hops; one in the **c** direction with $|\mu_c|/e = 2.959$ Å, the other in the **a** direction with $|\mu_a|/e = 4.594$ Å.

The other defects which are reasonable to consider are shown in Figs. 13(b) and 14. The polar behavior of these

[34] R. Haul and G. Dümbgen, J. Phys. Chem. Solids **26**, 1 (1965).
[35] J. van Keymeulen, Naturwiss. **45**, 56 (1958).
[36] J. Yamashita and T. Kurosawa, J. Phys. Soc. Japan **15**, 802 (1960).

defects may be discussed in the same way as previously, and is also summarized. The titanium interstitial pair is included, its presence in reduced rutile having been inferred from mechanical relaxation studies.

The **c**-only hop of an electron trapped by a Ti^{+3} interstitial associated with two (or one) trivalent impurity ions, Fig. 13, accounts well for peak II. It is likely that there may be some contribution to peak II from the **c**-only hop associated with the oxygen vacancy, Fig. 12(a). Peak II cannot be due to the **c**-only hop possible with oxygen vacancies alone, however, since the oxygen vacancies would be expected to become progressively more associated with two impurities than one as the concentration of the latter is increased. This renders the center inoperative, a behavior not observed. Furthermore, if it is assumed that increasing the impurity concentration increases the oxygen vacancy concentration correspondingly, and that peak II therefore increases, than it follows that a peak due to the oblique hop of the electron trapped by the oxygen vacancy, Fig. 12(a) would also increase.

The only peak observed with both an **a** and **c** component, peak I, behaves in the opposite way; it disappears on increasing the impurity content. Peak I, which has an **a** and **c** component in the ratio 3.0 (theoretical ratio 2.27), certainly has its origin in an oblique hop. Two simple centers can exhibit this behavior, the oxygen vacancy with one impurity Fig. 12(a), and the Ti^{+3} interstitial with one impurity Fig. 13(b). The evidence favors the explanation that peak I is due to the oblique hop associated with the oxygen vacancy rather than the titanium interstitial, viz., that the peak decreases with increasing impurity content. The Ti^{+3} interstitial center, should exhibit another peak observable in the **a** direction only, due to

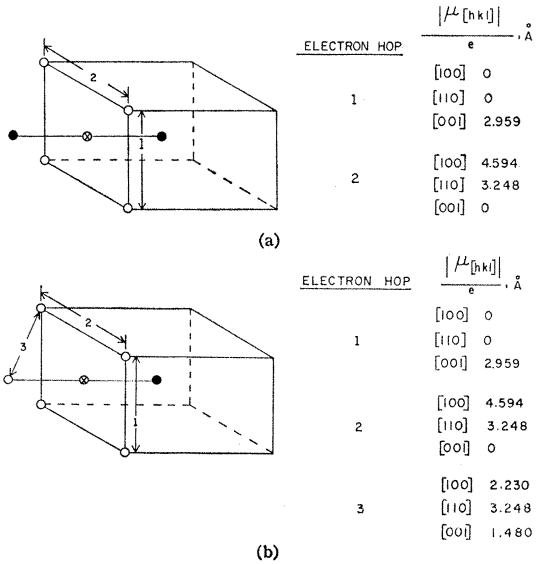

FIG. 13. Titanium interstitial with associated trivalent impurities. (a) With two impurities. (b) With one impurity.

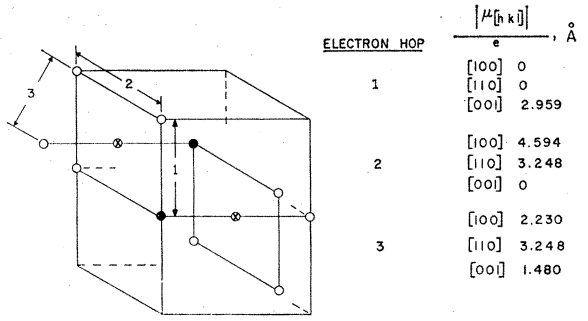

FIG. 14. Titanium di-interstitial associated with two trivalent impurities (Ref. 21).

the transition 2 in Fig. 13. The relaxation due to this process has not been observed. The actual hopping distance 4.594 Å, is the largest of all transitions considered, and it is reasonable to assume that this mode operates only at higher temperatures and is obscured by the surface phenomena then dominating the behavior. This explanation also involves the so far tacit assumption that the oblique hop involving the larger distance 3.570 Å, and to which peak I is ascribed, occurs at a lower temperature than the vertical shorter hop 2.959 Å which has been associated with peak II. The rate at which an electron hop occurs is strongly dependent on the overlap of the wave functions localized on each site. For the oxygen vacancy (Fig. 12) the perturbed-wave-function overlap in the now positive region previously occupied by the oxygen ion may be significantly larger than that associated with the Ti^{+3} interstitial center.

There are additional advantages in ascribing peak I to the oblique transition of oxygen vacancies. Granting that the (small) number of oxygen vacancies remains fixed (Haul and Dümbgen[34]) and that trivalent impurities preferentially associate with oxygen vacancies, then the rapid decrease of peak I with increasing impurity observed is to be expected. This quenching by addition of trivalent impurity is not expected however if Ti^{+3} interstitials were involved, since their concentration changes with reduction state. Another advantage in ascribing peak I to the oxygen vacancy is that, like the center proposed as responsible for peak II, the oxygen vacancy associated with one impurity can trap only one electron. Centers with two electrons may not exhibit sharp relaxations due to the correlated motion of the electrons. The above explanation that peak I be due to the oblique hop at the oxygen vacancy complex, requires that the oblique hop of the Ti^{+3} interstitial complex be not observable. There are two reasons why this may be so. A Ti^{+3} interstitial capable of an oblique hop can also trap two electrons, and the correlated motion of the electrons may suppress the otherwise expected relaxation. Alternatively, the hopping distance involved is quite large, 3.570 Å, and like the **a** hop of this center Fig. 13(b), the hop may occur at higher temperatures, where it is obscured by the surface capacitance.

Peak III is small in one specimen, large in another; its magnitude is independent of reduction state and trivalent impurity. The dipole moment associated with this process has both **a** and **c** components. A substitutional pentavalent impurity compensated by a Ti^{+3} ion on a normal lattice site is a simple model which adequately explains this dielectric relaxation. The possible hops are of the oblique type.

It is interesting to note that it is not necessary to introduce anywhere a complex ionic model in which pairing of the defects introduced by reduction need be assumed to account for any of the dielectric behavior reported here, as must be done to explain the internal friction behavior. There is no reason that the defects responsible for the dielectric relaxations should also be responsible for the mechanical relaxations. There is some consistency in that simple point defects are inadequate in both cases.

The proposed models involving electrons localized on normal Ti^{+4} sites adjacent to a positive point defect introduced by nonstoichiometry appear reasonable. There is strong experimental evidence which indicates that the trivalent impurity in the crystal associates with the defects introduced by reduction. The **c**-only hop on lattice sites surrounding a titanium interstitial with two (or more) associated impurities provides the best explanation for peak II. The oblique hop on lattice sites surrounding an oxygen vacancy with one associated trivalent impurity provides the best explanation for peak I. There is some ambiguity in this assignment. Peak I may be due to the oblique hop associated with the Ti^{+3} interstital but this identification does not lead to so satisfactory or consistent an interpretation. Electron hopping on normal sites around a pentavalent impurity accounts well for peak III.

CONCLUSION

Dielectric measurements have proved fruitful in elucidating some of the localized states in reduced rutile. In particular, at low temperatures, polarons have been observed hopping between normal cation sites in the region of low electrostatic potential about a positive ionic defect core. This indicates that consecutive intercationic electron hopping will contribute to dc impurity conduction in rutile at somewhat higher temperatures. Dielectric measurements should be useful in observing similar processes in other transition-metal oxides.

ACKNOWLEDGMENTS

The authors would like to express their sincere appreciation to William W. Scott and Dr. Jerome R. Long for useful discussions and for experimental assistance. Appreciation is also expressed to the Advanced Research Projects Agency of the Department of Defense for financial support.